Asian Journal of Chemistry; Vol. 37, No. 11 (2025), 2773-2780
ASIAN JOURNAL OF CHEMISTRY
https://doi.org/10.14233/ajchem.2025.33973

# Green Synthesis of Silver Nanoparticles using *Raphanus sativus* Water Extract for Enhanced Antimicrobial and Photocatalytic Activities

SANGEETA GUPTA[1], AMANPREET KAUR[1,*], NEHA BHATT[2], MAN VIR SINGH[3], MANSI RANI[1] and SHUBHANGEE AGARWAL[1]

[1]Department of Chemistry, School of Sciences, IFTM University, Moradabad-244102, India
[2]Department of Chemistry, Pt. L.M.S., Rishikesh Campus, Shri Dev Suman Uttarakhand Vishwavidyalay, Rishikesh-249201, India
[3]School of Applied and Life Sciences, Uttaranchal Institute of Technology, Uttaranchal University, Dehradun-248007, India

*Corresponding author: E-mail: amanpreet2225@gmail.com

*Received*: 2 May 2025 *Accepted*: 23 September 2025 *Published online*: 27 October 2025 AJC-22166

In this study, the biosynthesis of silver nanoparticles (AgNPs) was achieved using *Raphanus sativus* (radish) aqueous extract acted as both a reducing and stabilizing agent. The formation of AgNPs was confirmed through visual colour change and characterized by various spectroscopic and microscopic techniques. UV-Vis spectroscopy confirmed the successful synthesis of AgNPs with a distinct absorption peak at 432.054 nm. Fourier-transform infrared (FT-IR) spectroscopy revealed absorption bands indicative of phytoconstituents acting as capping agents. Field emission scanning electron microscopy (FESEM) provided morphological insights, while X-ray diffraction (XRD) analysis deter-mined an average crystalline size of 20.35 nm. The photocatalytic efficiency of biosynthesized AgNPs was evaluated by the breakdown of methylene blue dye molecules during UV light exposure. The DPPH and ABTS radical scavenging assays were used to assess antioxidant activity, yielding $IC_{50}$ values of 22.43 µg/mL and 30.54 µg/mL, respectively. The significant inhibitory effects were observed while assessing antibacterial efficacy against Gram-positive (*Listeria monocytogenes* and *Staphylococcus aureus)* and Gram-negative (*Escherichia coli* and *Pseudomonas aeruginosa*) bacteria. A significant, dose-dependent inhibitory effect was observed against all tested bacterial strains, as indicated by the zones of inhibition. Furthermore, the inhibition experiments for α-amylase and α -glucosidase demonstrated encouraging antidiabetic effects, yielding $IC_{50}$ values of 210 µg/mL and 185 µg/mL, respectively. Furthermore, the photocatalytic activity of the biosynthesized AgNPs was assessed using the degradation of methylene blue under light irradiation, confirming their potential application in environmental remediation. Overall, the study highlights the multifunctional properties of *Raphanus sativus*-mediated silver nanoparticles and their promising applications in biomedical and environmental fields.

**Keywords: Green synthesis, *Raphanus sativus*, AgNPs, Photocatalytic degradation, Biological activities.**

## INTRODUCTION

Nanotechnology, a field that integrates various scientific disciplines, focuses on the synthesis, design and application of materials at the nanoscale. This innovative area has paved the way for advancements across multiple sectors such as medi-cine, environmental science and agriculture [1]. Among various types of nanoparticles, silver nanoparticles (AgNPs) have attracted significant scientific attention because of their exceptional physico-chemical properties and extensive biological activities, which encompass antimicrobial, antioxidant, anti-inflammatory, anti-cancer and catalytic activities [2]. Nonetheless, traditional approaches for synthesizing AgNPs frequently utilize harmful chemicals, require significant energy and entail intricate processes, which raises concerns regarding environmental and biological safety [3]. As a result, there is a growing need for the advancement of eco-friendly, sustainable and green methods for synthesizing nanoparticles.

The biosynthesis of nanoparticles through plant mediation offers a compelling alternative to traditional chemical and physical methods, owing to its simplicity, cost-effectiveness and compatibility with the environment [4]. Plants serve as a natural reservoir of bioactive compounds, including flavonoids, alkaloids, terpenoids, phenolics and proteins, which can function as natural reducing, capping and stabilizing agents in the synthesis of nanoparticles [5]. The phytochemicals play

a crucial role in reducing metal ions and also affect the size, shape and biological functionality of the resulting nanoparticles. Among the numerous plants investigated, *Raphanus sativus* (commonly referred to as radish) has surfaced as a noteworthy candidate owing to its abundant phytochemical profile. *R. sativus* is a root vegetable that is extensively utilized globally due to its nutritional and medicinal properties. The composition includes a variety of phytoconstituents such as glucosinolates, flavonoids, phenolic acids, anthocyanins and essential vitamins, recognized for their strong antioxidant and therapeutic effects.

This study presents an eco-sustainable approach for the biosynthesis of silver nanoparticles, utilizing *R. sativus* water extract as a natural reducing and stabilizing agent [6]. The synthesized AgNPs underwent characterization through multiple techniques to verify their formation and assess their physico-chemical properties. Moreover, the biological activities of the biosynthesized AgNPs were thoroughly examined [7]. The antioxidant potential was evaluated through standard *in vitro* assays, including DPPH and ABTS radical scavenging methods, demonstrating the ability of the nanoparticles to neutralize free radicals and mitigate oxidative stress [8]. Alongside their antioxidant activity, the synthesized AgNPs were assessed for their antidiabetic potential *via* inhibition assays targeting α-amylase and α-glucosidase enzymes, which are essential in carbohydrate digestion and blood glucose regulation [9]. The findings underscore the potential application of these nanoparticles in addressing postprandial hyperglycemia, a significant issue for individuals with diabetes. The antimicrobial properties of the biosynthesized AgNPs were investigated against various Gram-positive and Gram-negative bacterial strains, in addition to certain fungal pathogens. The results indicated that the AgNPs exhibit considerable antimicrobial properties, implying their potential use in the devel-opment of innovative antimicrobial agents or coatings aimed at preventing microbial infections [10]. Furthermore, the photocatalytic performance of the AgNPs was evaluated through the examination of methylene blue dye degradation when subjected to light irradiation [11]. The findings demonstrated that the nanoparticles were capable of efficiently catalyzing the decomposition of organic pollutants, underscoring their promise in environmental remediation efforts like wastewater treatment [12]. This study offers an eco-friendly approach for synthesizing silver nanoparticles using *R. sativus* and delivers indepth insights into their diverse biological activities. The results indicate that *R. sativus*-mediated AgNPs may be valuable options for the biomedical, pharmaceutical and environmental uses, opening avenues for further exploration in plant-based nanotechnology.

## EXPERIMENTAL

Silver nitrate, methanol, ethanol, 2,2-diphenyl-1-picrylhydrazyl (DPPH), 2,2′-azino-*bis*(3-ethylbenzothiazoline-6-sulfonic acid) (ABTS), α-amylase enzyme, α-glucosidase enzyme, starch solution, *p*-nitrophenyl-α-D-glucopyranoside (pNPG), methylene blue dye, phosphate buffer solutions (PBS), sodium hydroxide, hydrochloric acid, nutrient agar/broth or Mueller-Hinton agar.

**Plant material and preparation of extract:** The leaves of *R. sativus* were collected from Gumkhal, Pauri Garhwal, India. Taxonomic identification and authentication of the plant material were conducted at the Department of Botany, School of Sciences, IFTM University, Moradabad, where a voucher specimen was also deposited for future reference. The collected leaves were thoroughly washed with distilled water to remove surface contaminants and subsequently dried under shade conditions at ambient room temperature. Once completely dried, the leaves were mechanically pulverized into a fine powder using an electric laboratory blender to facilitate further experimental use [13].

**Phytochemical analysis:** The phytochemical composition of *R. sativus* aqueous extract was preliminarily analyzed to identify the major bioactive constituents responsible for the reduction and stabilization of AgNPs. Standard qualitative phytochemical tests were conducted to detect the presence of various secondary metabolites. The extract tested positive for flavonoids, phenolic compounds, alkaloids, saponins, tannins, terpenoids and glycosides. Flavonoids and phenolic compounds, known for their strong reducing and antioxidant properties, are believed to play a crucial role in the biosynthesis and capping of silver nanoparticles. Alkaloids and saponins, on the other hand, may contribute to the stabilization and biological activities of the nanoparticles. The presence of tannins and terpenoids further enhances the reducing power of the extract and possibly influences the size and morphology of the nanoparticles [14,15].

**Green synthesis of silver nanoparticles:** The *R. sativus* extract and silver nitrate solution were mixed in a suitable ratio (*e.g.* 10 mL extract to 90 mL 1 mM $AgNO_3$ solution). The reaction mixture was stirred continuously at room temperature (or slightly warm, around 40-50 ºC) for 2-4 h. A visible colour changes from pale yellow to dark brown indicated the formation of silver nanoparticles. The reaction mixture was kept in dark (to avoid photoactivation) and monitored periodically. The synthesized nanoparticles were separated by centri-fugation at 10,000 rpm for 15-20 min. The pellet was collected, washed 2-3 times with distilled water and once with ethanol to remove any unbound phytochemicals. The purified silver nanoparticles were dried at 50-60 ºC and stored for further characterization [16].

**Characterization:** UV-Vis spectroscopy was performed using a Shimadzu UV-1800 spectrophotometer by measuring the absorbance between 300 and 800 nm. The FTIR spectrum was recorded with Thermo-Scientific Nicolet iS50 FTIR spectrometer in the wavenumber range of 4000 to 400 $cm^{-1}$. XRD measurements were performed using a diffractometer with a Cu*K*α radiation source (λ = 1.5406 Å) in the 2θ range of 20º to 80º. FESEM images were captured at various magnifications using a JEOL JSM-7610F to analyze the morphology, size, and uniformity of the biosynthesized silver nanoparticles.

### Antioxidant activity

**DPPH free radical scavenging assay:** For the DPPH (2,2-diphenyl-1-picrylhydrazyl) free radical scavenging assay of AgNPs synthesized using *R. sativus* water extract, a solution of DPPH radical (0.1 mM) in methanol was prepared and mixed with varying concentrations of the biogenic AgNPs

solution [17]. The reaction mixture was incubated in the dark for 30 min at room temperature. The decrease in absorbance of the DPPH solution was measured at 517 nm using a UV-Vis spectrophotometer. The percentage inhibition of DPPH free radicals was calculated using the formula:

$$\text{Inhibition } (\%) = \frac{A_{control} - A_{sample}}{A_{control}} \times 100 \quad (1)$$

where $A_{control}$ is the absorbance of the DPPH solution without nanoparticles and $A_{sample}$ is the absorbance after the addition of nanoparticles. The results were compared to a standard antioxidant (*e.g.* ascorbic acid) to assess the antioxidant activity of the AgNPs.

**ABTS free radical scavenging assay:** For the ABTS (2,2'-azino*bis*(3-ethylbenzothiazoline-6-sulfonic acid)) assay of AgNPs synthesized using *R. sativus* water extract, the $ABTS^{\bullet+}$ was generated by reacting 7 mM ABTS with 2.45 mM $K_2S_2O_8$ and allowing the mixture to stand in dark at room temperature for 12-16 h [18]. The resulting $ABTS^{\bullet+}$ solution was diluted with ethanol to an absorbance of 0.70 ± 0.02 at 734 nm. Different concentrations of the synthesized AgNPs were then added to the $ABTS^{\bullet+}$ solution and the decrease in absorbance was measured at 734 nm after 6 min of reaction. The percentage of ABTS radical scavenging activity was calculated using the formula given in eqn. 1.

**Antidiabetic activity:** Using the α-amylase and α-glucosidase assay, biosynthesized AgNPs were tested for their potential to prevent diabetes.

**Inhibition assay of α-amylase:** For the α-amylase inhibition assay of AgNPs synthesized using *R. sativus* water extract, a reaction mixture containing 0.5 mL of synthesized AgNPs at varying concentrations and 0.5 mL of α-amylase enzyme solution (1 U/mL) was prepared [19]. The mixture was incubated at 37 ºC for 15 min to allow enzyme-nanoparticle interaction. After incubation, 0.5 mL of a 1% starch solution was added and the mixture was further incubated at 37 ºC for 30 min. The reaction was terminated by adding 1 mL of dinitrosalicylic acid (DNS) reagent, followed by heating in a boiling water bath for 5 min. The absorbance of the resulting solution was measured at 540 nm using a UV-Vis spectrophotometer.

**Inhibition assay of α-glucosidase:** For the α-glucosidase inhibition assay, a reaction mixture was prepared by incubating 0.1 mL of the synthesized AgNPs at varying concentrations with 0.1 mL of α-glucosidase enzyme solution (1 U/mL) in phosphate-buffered saline (pH 6.8) for 15 min at 37 ºC. Following this, 0.1 mL of p-nitrophenyl-α-D-gluco-pyranoside (PNPG, 5 mM) was added as the substrate and the reaction was allowed to proceed for 30 min at 37 ºC [20]. The enzymetic activity was terminated by the addition of 1 mL of 0.2 M $Na_2CO_3$ solution and the hydrolysis of PNPG was quantified by measuring the absorbance of the released *p*-nitrophenol at 405 nm.

**Antibacterial activity:** To evaluate the antibacterial activity of biosynthesized AgNPs, a disc diffusion assay was performed [21]. The bacterial cultures (*S. aureus* and *L. monocytogenes*; *E. coli* and *P. aeruginosa*), were inoculated on nutrient agar plates and allowed to dry. Sterile filter paper discs were impregnated with different concentrations of the AgNPs and placed onto the inoculated agar plates. The plates were incubated at 37 ºC for 24 h. After incubation, the zones of inhibition around the discs were measured in millimeters. The antibacterial efficacy of the AgNPs was compared with a positive control (erythromycin) and a negative control (DMSO). The results were analyzed to determine the minimum inhibitory concentration (MIC) of the AgNPs and to assess their potential as antibacterial agents.

**Photocatalytic activity:** The photocatalytic activity of biosynthesized AgNPs was evaluated by testing their ability to degrade a model pollutant, such as methylene blue (MB), under UV light irradiation. In a typical experiment, a fixed concentration of AgNPs was dispersed in an aqueous solution of methylene blue and the mixture was stirred in the dark for 30 min to achieve adsorption equilibrium. The solution was then exposed to UV light (365 nm) for a predetermined period and the degradation of methylene blue was monitored by measuring the decrease in absorbance at 664 nm using a UV-Vis spectrophotometer. The photocatalytic degradation efficiency was calculated by comparing the absorbance of the solution before and after exposure to UV light. The rate of degradation was determined by applying the pseudo-first-order kinetic model to the concentration data [22].

**Statistical analysis:** Statistical analysis of biosynthesized AgNPs involved calculating mean values and standard deviations (SD) for each assay. One-way ANOVA followed by post-hoc tests (Tukey's) was used to compare differences between control and experimental groups, with statistical significance set at $p < 0.05$. Data analysis was performed using software such as SPSS or GraphPad Prism.

## RESULTS AND DISCUSSION

The extraction of *Raphanus sativus* leaf material with water solvent resulted in a yield of 56.14%. Extract underwent qualitative analysis to identify various phytochemical constituents that contribute to the reduction and stabilization of silver nanoparticles. The analysis indicated that the extract contains a high concentration of secondary metabolites, as detailed in Table-1. These compounds probably contribute to the reduction of silver ions and serve as capping agents, which helps to prevent the aggregation of nanoparticles and improves their stability [23]. Polar phytochemicals extracted with polar solvents are particularly influential in the synthesis of nanoparticles.

TABLE-1
SCREENING OF THE WATER EXTRACT OF *R. sativus* FLOWER FOR QUALITATIVE PHYTOCHEMICAL PROPERTIES

| Phytoconstituents | Water extract |
|---|---|
| Alkaloids | – |
| Flavonoids | + |
| Phenol | + |
| Saponins | + |
| Tannins | – |
| Triterpenoids | + |

**UV-visible spectral studies:** The addition of *R. sativus* leaf extracts to the silver nitrate solution resulted in a colour

change from pale yellow to reddish-brown after 3 h. This observation suggests the reduction of $Ag^+$ to $Ag^0$ nanoparticles, thereby confirming the biosynthesis of AgNPs [24]. The UV-vis spectra of AgNPs and the leaves water extract exhibited a distinct peak at approximately 432.054 nm or AgNPs synthesized from water extract of *R. sativus* leaf following 3 h of incubation (Fig. 1).

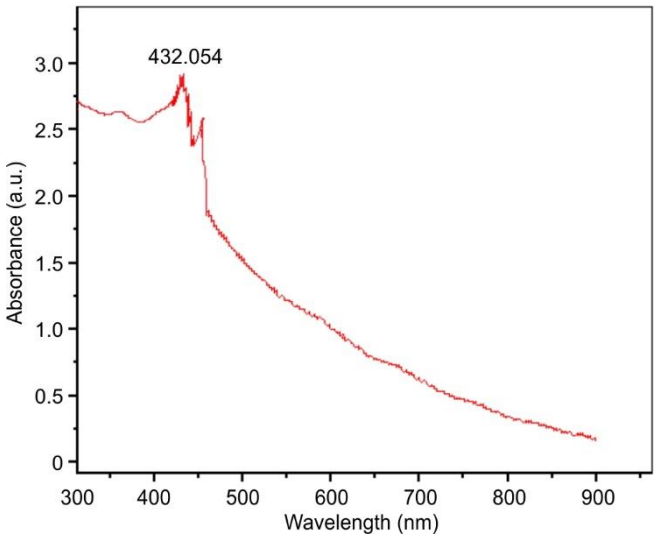


Fig. 1. UV-vis absorption spectra of biosynthesized AgNPs

**FTIR spectral studies:** The FTIR spectrum of biosynthesized AgNPs displayed significant absorption peaks at 3726.29, 3341.35, 2945.43, 2865.85, 2255.41, 1582.70, 1354.34, 1026.47, 901.54 and 811.35 $cm^{-1}$ (Fig. 2), suggesting the presence of phytoconstituents that function as capping agents. The FTIR spectra of *R. sativus* water extract, associated with the biosynthesized AgNPs, demonstrated notable shifts in these peaks, indicating the reduction, capping and stabilization of the nanoparticles. A shift at 3341.35 $cm^{-1}$ is associated with O–H or N–H stretching from phenolic compounds found in the leaf extract [25]. The peak observed at 2945.43 $cm^{-1}$ is indicative of C–H stretching associated with methylene or aliphatic groups, which is a characteristic of triterpenoid saponins. The band observed at 1582.70 $cm^{-1}$ is associated with the stretching of alkenyl or aromatic C=C bonds, while the band at 1354.34 $cm^{-1}$ signifies –C–O stretching typically found in phenols or tertiary alcohols. The band at 1015.59 $cm^{-1}$ is associated with O–H stretching in phenolic groups, while the band at 811.35 $cm^{-1}$ is linked to C–O and C–S stretching, commonly observed in aliphatic chloro compounds. The observed peaks are mainly associated with phenolic groups found in polyphenols, triterpenoids, alkaloids, steroids and tannins, which are prevalent in the leaf extract and play a significant role in the synthesis of green synthesized AgNPs.

**Powdered X-ray diffraction:** The XRD pattern of biosynthesized AgNPs revealed five distinct diffraction peaks at 2θ values of 27.45º, 34.35º, 36.84º, 40.15º, 46.78º, 48.53º, 50.78º and 58.10º (Fig. 3). The identified peaks align with the (100), (002), (101), (210), (122), (110), (220) and (311) planes, respectively, confirming the face-centered cubic (fcc) crystalline structure of the AgNPs. The size of the nanoparticles significantly influences the patterns observed in XRD peaks.

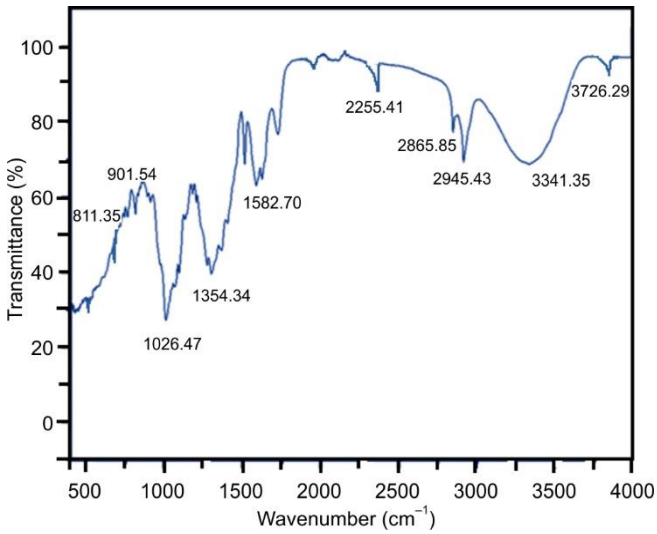


Fig. 2. FTIR spectra of biosynthesized AgNPs

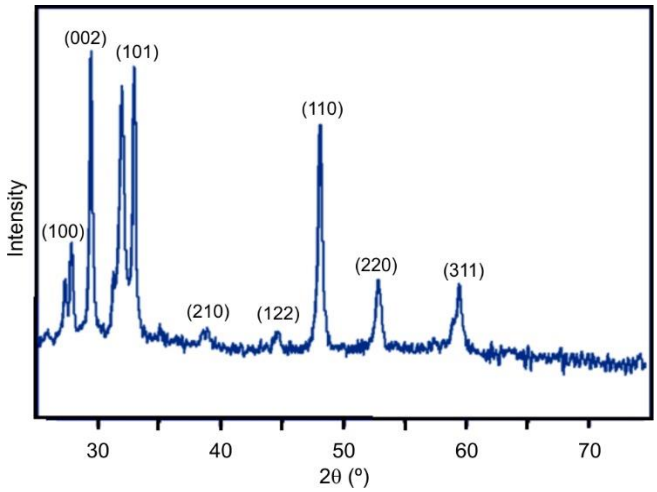


Fig. 3. XRD spectrum of biosynthesized AgNPs

The presence of different reducing agents in the leaves extract is essential for stabilizing the AgNPs and maintaining their crystalline structure, a feature also observed in other biosynthesized nanoparticles [26]. Table-2 presents the XRD analysis data of AgNPs synthesized using *R. sativus* leaf extract, confirming the distinct crystalline planes with an average crystallite size of 20.35 nm. The sharp diffraction peaks and *d*-spacing values indicate well-defined nanocrystalline particles.

TABLE-2
MILLER INDICES, FWHM VALUES, d-SPACING AND AVERAGE CRYSTALLITE SIZE CALCULATED OF AgNPs SYNTHESIZED FROM *R. sativus* LEAF WATER EXTRACT

| *hkl* | Pos. (º2θ) | FWHM Left (º2θ) | d-spacing (Å) |
|---|---|---|---|
| 100 | 27.5382 | 0.2449 | 2.75323 |
| 002 | 30.4832 | 0.3714 | 2.85753 |
| 101 | 33.4829 | 0.3494 | 2.37932 |
| 210 | 39.1530 | 0.3143 | 2.15684 |
| 122 | 45.7843 | 0.3978 | 1.95748 |
| 110 | 48.5134 | 0.3492 | 1.35983 |
| 220 | 52.7489 | 0.3635 | 1.85934 |
| 311 | 58.1012 | 0.5502 | 1.23544 |
| Average crystallite size 20.35 nm | | | |

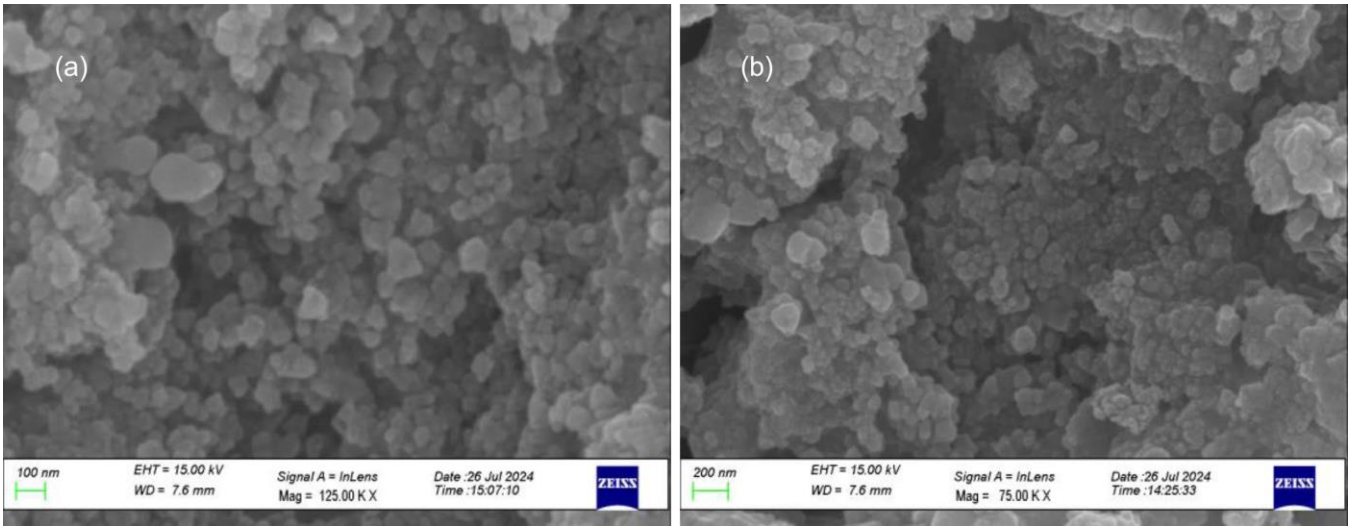


Fig. 4. FESEM images of AgNPs synthesized from *R. sativus* leaf water extract

**SEM studies:** The morphology of the green-synthesized AgNPs was examined through scanning electron microscopy (SEM). The AgNPs exhibited a range of shapes such as irregular, granulated and ellipsoidal forms, with some aggregation (Fig. 4). The SEM analysis revealed that the size of the AgNPs ranged from 30 to 50 nm. The microscopic examination indicated that the nanoparticles exhibited a predominantly spherical shape and were evenly distributed throughout the sample. The significant agglomeration of the AgNPs can be linked to the dehydration process that occurred during the sample preparation for SEM analysis [27].

**Antioxidant activity:** The antioxidant activity of the biosynthesized AgNPs was evaluated *in vitro* through the DPPH and ABTS assays. The findings indicated a concentration-dependent enhancement in the scavenging activity of AgNPs on DPPH and ABTS radicals (Fig. 5). Ascorbic acid functioned as a positive control. Biosynthesized AgNPs demonstrated superior free radical inhibition, showing $IC_{50}$ values of 22.43 and 30.54 µg/mL for DPPH and ABTS assays, respectively, in contrast to the standard ascorbic acid, which had $IC_{50}$ values of 9.23 and 11.29 µg/mL. The nanoparticles demonstrated stable neutral radical quenching from DPPH and cationic radical scavenging from ABTS. The DPPH assay demonstrated the capacity of AgNPs to transfer electrons and neutralize free radicals, whereas the ABTS assay revealed the participation of both electron and hydrogen transfer mechanisms in the scavenging of cationic free radicals [28].

**Antidiabetic activity:** The *in vitro* inhibitory activity of biosynthesized AgNPs on α-amylase and α-glucosidase was evaluated in comparison to acarbose, as illustrated in Fig. 6. The $IC_{50}$ value for AgNPs was determined to be 210 µg/mL respectively, demonstrating significant α-amylase inhibitory activity. In a similar manner, the *in vitro* inhibitory activity of AgNPs on α-glucosidase was assessed in comparison to acarbose (Fig. 6). The variation in α-glucosidase inhibition across various sample concentrations facilitated the estimation of $IC_{50}$ values for both AgNPs and acarbose. The biosynthesized AgNPs was demonstrated significant α-glucosidase inhibitory activity with an $IC_{50}$ value of 185 µg/mL respectively.

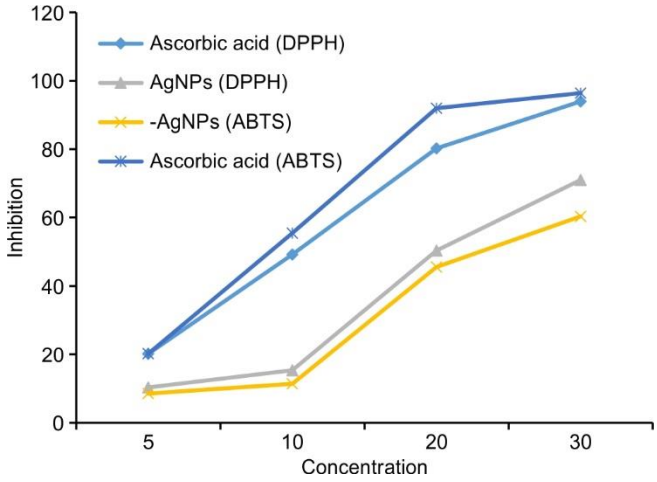


Fig. 5. Antioxidant activity by ABTS and DPPH method of AgNPs synthesized from water extract

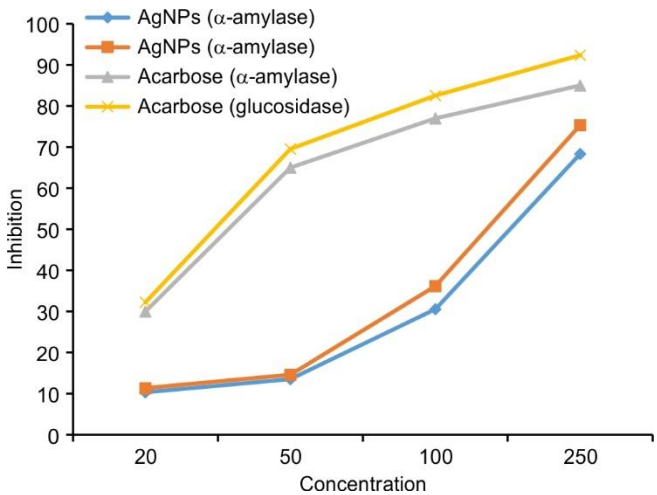


Fig. 6. Antidiabetic activity by α-amylase and α-glucosidase method of AgNPs synthesized from water extract

**Antibacterial activity:** The evaluation of the antibacterial activity was conducted through the disc diffusion method, targeting both Gram-positive bacteria (*S. aureus* and *L.*

TABLE-3
ZONE OF INHIBITION OF AgNPs SYNTHESIZED FROM *R. sativus* PEEL EXTRACT AT DIFFERENT CONCENTRATION

| Controls | Conc. (µg/mL) | *L. monocytogen* | *S. aureus* | *E. coli* | *P. aeruginosa* |
|---|---|---|---|---|---|
| AgNPs | 50 | 8.0 ± 0.46 | 9.0 ± 0.20 | 9.0 ± 0.00 | 10.10 ± 0.10 |
| | 100 | 12.01 ± 0.26 | 10.3 ± 0.55 | 11.18 ± 0.05 | 13.54 ± 0.54 |
| | 150 | 15.5 ± 0.02 | 17.3 ± 0.01 | 16.45 ± 0.10 | 18.12 ± 0.22 |
| Erythromycin | (10 µg/mL) | 12.45 ± 0.26 | 12.5 ± 0.10 | 17.7 ± 0.15 | 18.5 ± 0.10 |
| Norfloxacin | (10 µg/mL) | 11.47 ± 0.35 | 12.5 ± 0.10 | 14.7 ± 0.15 | 16.5 ± 0.10 |

*monocytogenes*) and Gram-negative bacteria (*E. coli* and *P. aeruginosa*). The biosynthesized AgNPs was demonstrated notable antibacterial efficacy, especially towards *S. aureus* and *P. aeruginosa*, with inhibition zones recorded at 17 mm and 18 mm, respectively, at the maximum concentration (Table-3). The antibacterial efficacy of AgNPs tends to be more significant in Gram-negative bacteria, likely attributable to variations in the structure of their cell walls [29].

**Photocatalytic activity:** The absorption spectra under UV light revealed the breakdown of methylene blue dye using biosynthesized AgNPs as photocatalyst is shown in Fig. 7. The reduction in absorbance at 664 nm over time indicates that AgNPs are successfully facilitating the degradation process. A degradation efficiency for AgNPs was 69% during 80 min for AgNPs derived from water extract. The photocatalytic activity of the nanoparticles can be explained by examining their surface area, morphology and crystallinity. Improving the crystallinity and surface area of the material leads to enhanced photocatalytic performance, subsequently influencing the overall degradation efficiency [30].

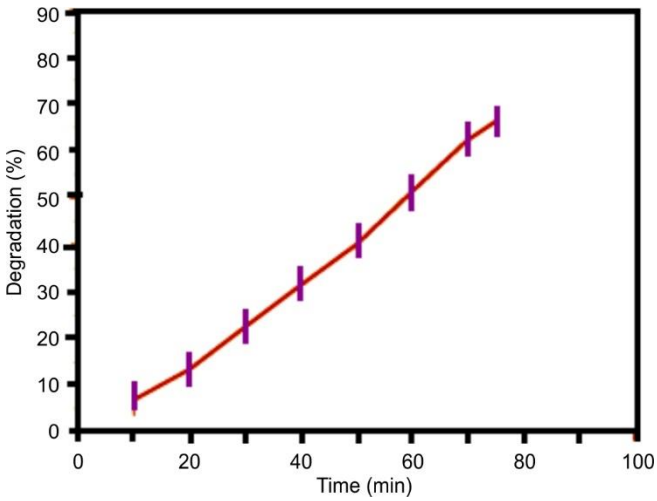


Fig. 7. Percentage degradation of irradiation time *vs.* methylene blue dye in the presence of biosynthesized AgNPs

**Comparative study:** The comparative data in Table-4 highlights the growing prominence of plant-mediated green synthesis of AgNPs as a viable and sustainable alternative to the conventional chemical and physical methods. Across the diverse plant sources like *Azadirachta indica*, *Moringa oleifera*, *Curcuma longa* and *Allium sativum*, the biosynthesized AgNPs predominantly exhibit spherical morphology with size ranges between 5-50 nm, which is consistent with the controlled nucleation and growth mediated by plant phytochemicals. The biological activities particularly the antimicrobial, antioxidant, anti-inflammatory, and cytotoxic effects affirm the therapeutic potential of these biosynthesized AgNPs. Particularly, *Allium sativum* and *Zingiber officinale* derived AgNPs demonstrated broad-spectrum antibacterial and antifungal efficacy, whereas *Curcuma longa* and *Camellia sinensis* based AgNPs exhibited promising anticancer and antioxidant activities. These bioactivities are often attributed to the small size and high surface area-to-volume ratio of AgNPs, facilitating interaction with microbial membranes and oxidative stress pathways. In addition to the biomedical relevance, several plant-mediated AgNPs also showed photocatalytic applications such as dye degradation (*e.g.* methylene blue, textile dyes), environmental pollutant removal and water purification emphasizing their multifunctionality and value in environmental remediation. For instance, *Moringa oleifera* and *Ocimum sanctum* extracts facilitated AgNPs synthesis with prominent dye degradation capacity, illustrating their potential in wastewater treatment.

The present study utilizing *R. sativus* aqueous extract resulted in well-dispersed and stable AgNPs with controlled morphology likely influenced by the presence of glucosinolates, isothiocyanates and phenolics compounds naturally found in *R. sativus*. Functionally, the *R. sativus*-mediated AgNPs displayed strong antimicrobial and antioxidant activities, comparable to or exceeding those reported in other plant systems. This strengthens the potential of *R. sativus* as a viable candidate for the biomedical applications including antimicrobial coatings, wound dressings and antioxidant therapies. Moreover, the synthesis process adhered to green chemistry principles utilizing water as a solvent, renewable plant waste, and ambient reaction conditions leading to reduced environmental footprint and enhanced atom economy.

## Conclusion

In this work, silver nanoparticles (AgNPs) synthesized using *Raphanus sativus* water extract demonstrated promising properties in various applications, including antioxidant, antibacterial and enzymatic inhibition activities. The biosynthesized AgNPs exhibited significant DPPH and ABTS radical scavenging abilities, highlighting their potential as effective natural antioxidants. Moreover, the biosynthesized AgNPs showed considerable antibacterial activity against common pathogens and effectively inhibited α-amylase and α-glucosidase enzymes, suggesting their potential for use in managing diabetes. The photocatalytic degradation of pollutants, such as methylene blue dye, further confirmed their utility in environmental remediation. These findings indicate that AgNPs synthesized *via* green methods using *R. sativus* extract are a sustainable and versatile material with significant biomedical and environmental applications.

TABLE-4
COMPARATIVE OVERVIEW OF DIFFERENT PLANTS-DERIVED SILVER NANOPARTICLES: NANOSTRUCTURE PROPERTIES, BIOLOGICAL ACTIVITY, AND PHOTOCATALYTIC APPLICATIONS

| Plant source | Extract type | Size/shape of AgNPs | Reported biological activity | Photocatalytic/other applications | Ref. |
|---|---|---|---|---|---|
| *Azadirachta indica* | Leaf extract | 10-40 nm, spherical | Highly effective antibacterial properties against *E. coli* and *S. aureus* | Methylene blue degradation | [31] |
| *Moringa oleifera* | Leaf extract | 20-50 nm, mostly spherical | Effects related to antioxidants and cytotoxicity | Photocatalytic activity against textile dyes | [32] |
| *Aloe vera* | Leaf gel extract | 15-35 nm, spherical | Fungal and bacterial resistance | Employed in the process of purifying water | [33] |
| *Curcuma longa* | Rhizome extract | 12-30 nm, spherical | Potential for antioxidant and anticancer properties | Photocatalytic dye degradation | [34] |
| *Ocimum sanctum* | Leaf extract | 8-25 nm, spherical | Substances that combat microbes and reduce inflammation | Environmental pollutant degradation | [35] |
| *Camellia sinensis* | Leaf extract | 15-40 nm, triangular and spherical | Properties related to antioxidants and anticancer effects | Catalysis and photocatalysis of dyes | [36] |
| *Zingiber officinale* | Rhizome extract | 10-30 nm, spherical | Antibacterial and antifungal | Applications in the biomedical field | [37] |
| *Allium sativum* | Bulb extract | 5-20 nm, spherical | Antibacterial against Gram-positive and Gram-negative strains | Possible applications in food preservation and medicine | [38] |
| *Mentha piperita* | Leaf extract | 18-35 nm, spherical | Antioxidant and antimicrobial | Dye degradation and pharmaceutical applications | [39] |

## ACKNOWLEDGEMENTS

The authors express their gratitude to the Department of Chemistry, IFTM University and University Science Instrumentation Centre at Delhi University, for providing the spectral characterization facilities.

## CONFLICT OF INTEREST

The authors declare that there is no conflict of interests regarding the publication of this article.

## REFERENCES

1. A. Waris, M. Din, A. Ali, M. Ali, S. Afridi, A. Baset and A.U. Khan, *Inorg. Chem. Commun.*, **123**, 108369 (2021); https://doi.org/10.1016/j.inoche.2020.108369.
2. K.S. Siddiqi, A. Husen and R.A.K. Rao, *J. Nanobiotechnol.*, **16**, 14, (2018); https://doi.org/10.1186/s12951-018-0334-5
3. A. Singh, P.K. Gautam, A. Verma, V. Singh, P.M. Shivapriya, S. Shivalkar, A.K. Sahoo and S.K. Samanta, *Biotechnol. Rep.*, **25**, e00427 (2020); https://doi.org/10.1016/j.btre.2020.e00427
4. S.C. Mali, A. Dhaka, C.K. Githala and R. Trivedi, *Biotechnol. Rep.*, **27**, e00518 (2020); https://doi.org/10.1016/j.btre.2020.e00518
5. S. Ying, Z. Guan, P.C. Ofoegbu, P. Clubb, C. Rico, F. He and J. Hong, *Environ. Technol. Innov.*, **26**, 102336 (2022); https://doi.org/10.1016/j.eti.2022.102336
6. H. Agarwal, A. Nakara and V.K. Shanmugam, *Biomed. Pharmacother.*, **109**, 2561 (2019); https://doi.org/10.1016/j.biopha.2018.11.116
7. D. Bamal, A. Singh, G. Chaudhary, M. Kumar, M. Singh, N. Rani, P. Mundlia and A.R. Sehrawat, *Nanomaterials*, **11**, 2086 (2021); https://doi.org/10.3390/nano11082086
8. L.M. Anaya-Esparza, Z.V.D.L. Mora, O. Vázquez-Paulino, F. Ascencio and A. Villarruel-López, *Molecules*, **26**, 5341 (2021); https://doi.org/10.3390/molecules26175341
9. A. S. González-Garibay, O. R. Torres-González, I. M. Sánchez- Hernández and E. Padilla-Camberos, *Pharmaceuticals*, **18**, 1412 (2025); https://doi.org/10.3390/ph18091412
10. S.I. Hamdallah, R. Zoqlam, P. Erfle, M. Blyth, A.M. Alkilany, A. Dietzel and S. Qi, *Int. J. Pharm.*, **584**, 119408 (2020); https://doi.org/10.1016/j.ijpharm.2020.119408
11. G.A. Marcelo, C. Lodeiro, J.L. Capelo, J. Lorenzo and E. Oliveira, *Mater. Sci. Eng. C*, **106**, 110104 (2020); https://doi.org/10.1016/j.msec.2019.110104
12. A.G. Niculescu, C. Chircov and A.M. Grumezescu, *Methods*, **199**, 16 (2022); https://doi.org/10.1016/j.ymeth.2021.04.018
13. M.C. Uribe-López, M.C. Hidalgo-López, R. López-González, D.M. Frías-Márquez, G. Núñez-Nogueira, D. Hernández-Castillo and M.A. Alvarez-Lemus, *J. Photochem. Photobiol. Chem.*, **404**, 112866 (2021); https://doi.org/10.1016/j.jphotochem.2020.112866
14. M. Sajid and J. Płotka-Wasylka, *Microchem. J.*, **154**, 104623 (2020); https://doi.org/10.1016/j.microc.2020.104623
15. N.A. Patil, S. Udgire, D.R. Shinde and P.D. Patil, *Chem. Methodol.*, **7**, 15 (2023); https://doi.org/10.22034/chemm.2023.355289.1597
16. J.S. Boruah, C. Devi, U. Hazarika, P.V. Bhaskar Reddy, D. Chowdhury, M. Barthakur and P. Kalita, *RSC Adv.*, **11**, 28029 (2021); https://doi.org/10.1039/D1RA02669K
17. T.U. Rahman, H. Khan, W. Liaqat and M.A. Zeb, *Microsc. Res. Tech.*, **85**, 202 (2022); https://doi.org/10.1002/jemt.23896
18. A. Shukla, A. Kaur and R.K. Shukla, *Indian Drugs*, **58**, 42 (2021); https://doi.org/10.53879/id.58.04.12201
19. A. Kaur, M.V. Singh, N. Bhatt, S. Arora and A. Shukla, *ES Food Agroforest.*, **15**, 1068 (2023); https://doi.org/10.30919/esfaf1068
20. A. Shukla, A. Kaur, R.K. Shukla and Anchal, *Res. J. Pharm. Technol.*, **12**, 1811 (2019); https://doi.org/10.5958/0974-360X.2019.00302.0
21. A. Kaur, A. Shukla and R.K. Shukla, *Indian J. Nat. Prod. Resour.*, **12**, 538 (2022).
22. P. Pokhriyal, A. Kaur, A. Shukla, S. Dhiman and H. Gupta, *Russ. J. Bioorgan. Chem.*, **50**, 408 (2024); https://doi.org/10.1134/S1068162024020158
23. A. Fouda, A.M. Eid, E. Guibal, M.F. Hamza, S.E.D. Hassan, D.H.M. Alkhalifah and D. El-Hossary, *Appl. Sci.*, **12**, 12879 (2022); https://doi.org/10.3390/app122412879
24. S.A. Khan, S. Shahid and C.S. Lee, *Biomolecules*, **10**, 835 (2020); https://doi.org/10.3390/biom10060835

25. B. Boro, J.S. Boruah, C. Devi, Alemtoshi, B. Gogoi, P. Bharali, P.V.B. Reddy, D. Chowdhury and P. Kalita, *J. Mol. Struct.*, **1300**, 137227 (2024); https://doi.org/10.1016/j.molstruc.2023.137227
26. E.V. Kumar, B.S. Niveditha, L. Sushmitha, B.K. Usha, B.E.K. Swamy, Anitha and G. Nagaraju, *Nano-Struct. Nano-Objects*, **36**, 101066 (2023); https://doi.org/10.1016/j.nanoso.2023.101066
27. S.A. Korde, P.B. Thombre, S.S. Dipake, J.N. Sangshetti, A.S. Rajbhoj and S.T. Gaikwad, *Inorg. Chem. Commun.*, **153**, 110777 (2023); https://doi.org/10.1016/j.inoche.2023.110777
28. F. Barzegarparay, H. Najafzadehvarzi, R. Pourbagher, H. Parsian, S.M. Ghoreishi and S. Mortazavi-Derazkola, *Biomass Convers. Biorefin.*, **14**, 25369 (2024); https://doi.org/10.1007/s13399-023-04604-z
29. H. Baloch, A. Siddiqua, A. Nawaz, M.S. Latif, S.Q. Zahra, S.Y. Alomar, N. Ahmad and T.M. Elsayed, *Gels*, **9**, 284 (2023); https://doi.org/10.3390/gels9040284
30. A. Sati, T.N. Ranade, S.N. Mali, H.K. Ahmad Yasin and A. Pratap, *ACS Omega*, **10**, 7549 (2025); https://doi.org/10.1021/acsomega.4c11045
31. S. Ahmed, Saifullah, M. Ahmad, B.L. Swami and S. Ikram, *J. Radiat. Res. Appl. Sci.*, **9**, 1 (2016); https://doi.org/10.1016/j.jrras.2015.06.006
32. H. Perumalsamy, S.R. Balusamy, J. Sukweenadhi, S. Nag, D.M. Ali, M. El-Agamy Farh, H. Vijay and S. Rahimi, *J. Nanobiotechnol.*, **22**, 71 (2024); https://doi.org/10.1186/s12951-024-02332-8
33. T.R. Anju, S. Parvathy, M. Valiya Veettil, J. Rosemary, T.H. Ansalna, M.M. Shahzabanu and S. Devika, *Mater. Today Proc.*, **43**, 3956 (2021); https://doi.org/10.1016/j.matpr.2021.02.665
34. A. Gangal, N.K. Sethiya, M. Duseja, R.K. Shukla, D. Bisht, V.S. Rana, H. Lalhlenmawia, S. Azizov and D. Kumar, *Green Chem. Lett. Rev.*, **18**, 2449122 (2025); https://doi.org/10.1080/17518253.2024.2449122
35. A.K. Singh, *Bioresour. Technol. Rep.*, **19**, 101118 (2022); https://doi.org/10.1016/j.biteb.2022.101118
36. F. Göl, A. Aygün, A. Seyrankaya, T. Gür, C. Yenikaya and F. Şen, *Mater. Chem. Phys.*, **250**, 123037 (2020); https://doi.org/10.1016/j.matchemphys.2020.123037
37. N.S. Al-Radadi, Abdullah, S. Faisal, A. Alotaibi, R. Ullah, T. Hussain, M. Rizwan, Saira, N. Zaman, M. Iqbal, A. Iqbal and Z. Ali, *Inorg. Chem. Commun.*, **140**, 109274 (2022); https://doi.org/10.1016/j.inoche.2022.109274
38. K. Velsankar, R.M.A. Kumar, R. Preethi, V. Muthulakshma and S. Sudhahar, *J. Environ. Chem. Eng.*, **8**, 104123 (2020); https://doi.org/10.1016/j.jece.2020.104123
39. Z. Hussain, M. Jahangeer, A. Sarwar, N. Ullah, T. Aziz, M. Alharbi, A. Alshammari and A.F. Alasmari, *J. Chil. Chem. Soc.*, **68**, 5865 (2023); https://doi.org/10.4067/s0717-97072023000205865